Polymer Chemistry

Accepted Manuscript

This article can be cited before page numbers have been issued, to do this please use: W. Ceunen, A. Van Oosten, R. Vleugels, T. Verbiest, J. De Winter, P. Gerbaux, Z. Li, S. De Feyter and G. Koeckelberghs, *Polym. Chem.*, 2018, DOI: 10.1039/C8PY00393A.

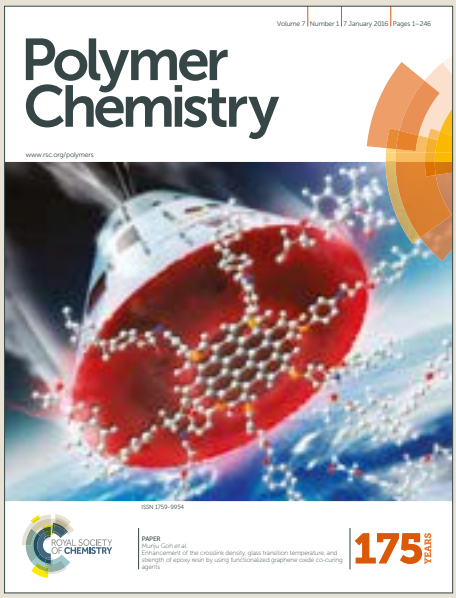

ROYAL SOCIETY OF CHEMISTRY

rsc.li/polymers

ROYAL SOCIETY OF CHEMISTRY
View Article Online
DOI: 10.1039/C8PY00393A

Journal Name

ARTICLE

Synthesis and supramolecular organization of chiral poly(thiophene)-magnetite hybrid nanoparticles

Received 00th January 20xx,
Accepted 00th January 20xx

DOI: 10.1039/x0xx00000x

www.rsc.org/

Ward Ceunen,[a] Annelien Van Oosten,[a] Rick Vleugels,[b] Julien De Winter,[c] Pascal Gerbaux,[c] Zhi Li,[d] Steven de Feyter,[d] Thierry Verbiest[b] and Guy Koeckelberghs*[a]

In this study, poly((*S*)-3-(3',7'-dimethyloctyl)thiophene) is synthesized via KCTCP, using a catechol-based external Ni-initiator. After characterization, the polymer's catechol functionality is deprotected and coupled with magnetite nanoparticles and the supramolecular organization is studied using UV/Vis, CD, AFM and Faraday measurements. We conclude that no long range supramolecular ordering is present in the hybrid material and that only interchain interactions between polymer chains attached on different nanoparticles are present. Also the effect of the new initiator and the branched monomer side chain on the controlled character of the KCTCP is investigated. It is found that a methyl group on the 3-position of the monomer sidechain already affects the controlled character of the polymerization. Also, a mechanism for the observed effects of the branched monomer and the new catechol-based initiator on the controlled character of the polymerization is proposed.

INTRODUCTION

Apart from the nature of the polymer e.g. it's molecular structure, the properties of polymeric devices also greatly depend on the supramolecular architecture, governed by interchain interactions, molar mass, regioregularity, dispersity and so forth. For conjugated polymers (CP's), extensive research towards their supramolecular structure is already conducted for homopolymers and block copolymers[1], but for more advanced (hybrid) nanostructures, far less information is available. Nevertheless, these studies are of utmost importance to improve the performance of polymeric materials, such as hybrid photovoltaics, which have an enormous potential to be used in low-cost, light-weight and flexible devices for the production of green energy.[2] In these materials the excellent processability and optoelectronic properties of conjugated polymers are combined with the size-dependent optical properties, high electron mobility and physical and chemical stability of inorganic nanoparticles (NP's) to form intermixing nanostructured networks.[2] In short, these devices rely on the transport of electron-hole pairs (excitons) through the material to the organic-inorganic interface, avoiding recombination.[3] At this interface, the charges are separated before migrating towards their respective electrodes. The efficiency of this process greatly depends on the interaction between the different polymer chains and the coupling with the other components of the device. Nowadays several of these systems reach efficiencies around 6%.[4] Two important issues stalling further progress are (1) the quality of the organic-inorganic interface, which is crucial for a good charge separation and (2) the supramolecular organization, which influences the homogeneity of the blend. To take on this first challenge, polymers can be equipped with functional groups that couple robustly to the inorganic nanoparticles, to obtain a more homogeneous and stable CP-NP blend. Few examples exist, for instance amine[5], thiol[6], pyridine[7], cyanoacrylic acid[8], trialkoxysilane[9] or catechol[10,11] groups, but in most cases, although providing a better interfacial interaction, the linker used also hinders charge transfer due to its non-conductive character. Both (1) and (2) (via a catechol group) will be subjects of this paper.

In this paper, we study the supramolecular organization of hybrid materials, consisting of chiral poly((*S*)-3-(3',7'-dimethyloctyl)thiophene), covalently coupled to magnetite nanoparticles. Poly(3-alkylthiophene) is the benchmark polymer for these systems, due to its good environmental stability, processability and modifiability.[1] Also, years of research in this field allow for the synthesis of well-defined, tailor-made polymers via techniques such as the controlled Kumada Catalyst Transfer Condensative Polymerization (KCTCP) and external Ni-initiation.[1] Via KCTCP, a polymer with a low dispersity and a predesigned molar mass and end-groups can be obtained. The selected polymer bearing chiral sidechains will allow for a study of the supramolecular organization via CD measurements, in addition to UV/Vis spectroscopy, atomic force microscopy (AFM) and Faraday measurements. Further, since every growing polymer chain

[a] *Laboratory for Polymer Synthesis, Department of Chemistry, KU Leuven, Celestijnenlaan 200F, 3001 Heverlee, Belgium.*
[b] *Molecular Imaging and Photonics, Department of Chemistry, KU Leuven, Celestijnenlaan 200D, 3001 Leuven, Belgium.*
[c] *Organic Synthesis and Mass Spectrometry Laboratory, Interdisciplinary Center for Mass Spectrometry, University of Mons-UMONS, Place du Parc 23, 7000 Mons, Belgium.*
[d] *Division of Molecular Imaging and Photonics, Department of Chemistry, KU Leuven, Celestijnenlaan 200F, 3001 Heverlee, Belgium.*
† Electronic Supplementary Information (ESI) available: Used instrumentation and experimental details as well as ^{1}H NMR, ^{31}P NMR, CD and UV/Vis spectra, MALDI-ToF spectra and TEM results. See DOI: 10.1039/x0xx00000x

originates from the external initiator, a catechol functionality will be directly attached to each polymer chain.[12] This catechol group will guarantee a conductive[8,13,14] and stable coupling to the magnetite nanoparticles[15], and potentially also to various other types of nanoparticles such as CdS[14], CdSe[14], TiO_2[10], and ZnO[16], which are commonly used in the synthesis of hybrid photovoltaics.[6,8,17] Since it's the shape, rather than the nature of the nanoparticle that predominantly influences the supramolecular ordering of the hybrid system, magnetite can be used as a 'dummy' nanomaterial. Finally, the use of superparamagnetic magnetite nanoparticles allows for a simple purification of the obtained hybrid material by means of magnetic decantation.

Results and discussion

In this study, poly((*S*)-3-(3',7'-dimethyloctyl)thiophene) is synthesized via KCTCP, using a catechol-based external Ni-initiator (**cat**). After characterization, the polymer's catechol functionality is deprotected for subsequent coupling with magnetite nanoparticles. Finally, to study the supramolecular organization, a well-defined material, with solely the targeted end-groups, is required. Therefore, we first investigate to which extend the controlled character of the KCTCP is preserved when polymerizing the branched (+)-(*S*)-2-bromo-5-chloromagnesio-3-(3,7-dimethyloctyl)-thiophene (**3DMOT**) monomer or when using the new **cat.** initiator. For this purpose ***o*-tol.-P3DMOT**, **cat.-P3HT** and **cat.-P3DMOT** are synthesized using 2-bromo-5-chloromagnesio-3-hexylthiophene (**3HT**), **3DMOT**, ***o*-tol.** and **cat.**. (Fig. 1)

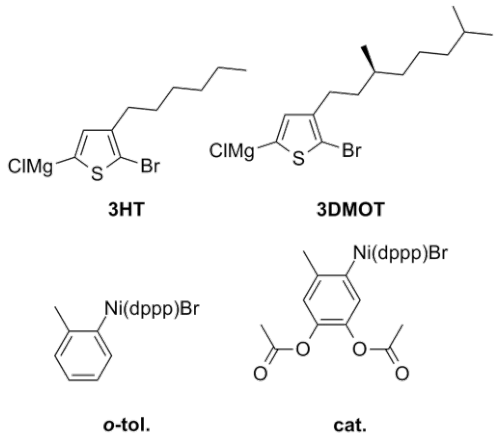

Fig. 1 The monomers and external initiators.

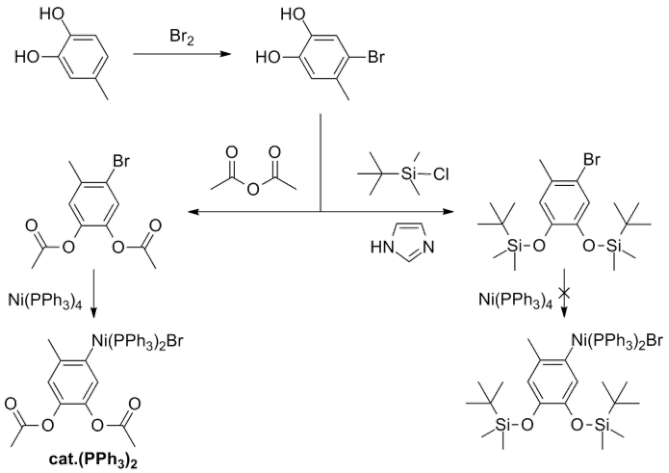

Fig. 2 Synthesis of the external initiator.

Synthesis of the precursor initiators. The external Ni-precursor initiators are synthesized via the insertion of $Ni(PPh_3)_4$ into the corresponding functionalized aryl bromide.[12] Similar to earlier synthesized phenol based Ni-initiators, to protect the catechol hydroxyl functionalities during the polymerization, *t*-butyl dimethylsilyl ethers were initially employed, but the obtained aryl bromide proved to be too electron-rich to undergo oxidative insertion. Instead, the catechol functionality is acetylated in order to reduce the electron density of the C-Br bond so that a suitable initiator could be prepared. (Fig. 2)

Synthesis of the monomers and polymers. The synthesis of the monomers is conducted as reported in literature (Fig. 3).[18] All polymers in this study are synthesized via KCTCP[1] and purified via fractionation using methanol and chloroform. The molar masses and dispersities are analyzed using standard GPC and ^{1}H NMR spectroscopy.[19] In a typical polymerization experiment, THF-solutions of initiator are stirred in several glass tubes for 20 minutes, together with 2 eq. of 1,3-bis(diphenylphosphino)propane (dppp). Parallel with this ligand exchange, the precursor monomer undergoes a Grignard metathesis (GRIM) reaction for 30 minutes in THF, induced by the addition of 1 eq. of *i*-propylmagnesium chloride.lithiumchloride. To initiate the polymerization, different volumes of this monomer solution are cannulated to the initiator solutions. After full conversion, the polymerization is terminated by adding HCl in THF. (Fig. 4)

Influence of the branched side chain. To investigate the influence of the branched monomer on the controlled character of the polymerization, a series of ***o*-tol.-P3DMOT** is synthesized from

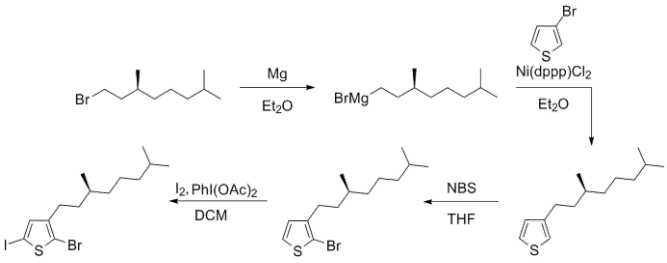

Fig. 3 The monomer synthesis.

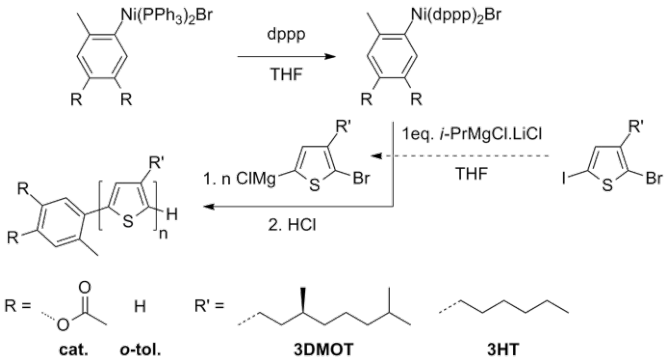

Fig. 4 General overview of a polymerization experiment.

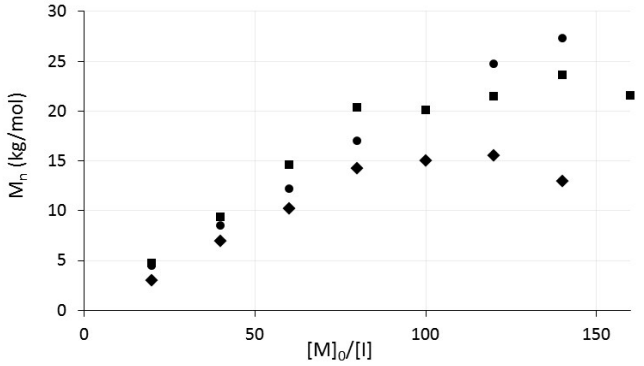

Fig. 5 GPC-obtained M_n *vs* $[M]_0/[I]$ for ***o*-tol.-P3DMOT** (■), **cat.-P3HT**(●) and **cat.-P3DMOT** (♦).

polymerization and, as a consequence ***o*-tol.-P3HT**, synthesized from **3HT** with ***o*-tol.**, shows a linear correlation between the GPC-measured M_n and $[M]_0/[I]$ until at least 35 kg/mol.[20] For the obtained ***o*-tol.-P3DMOT**, the results are shown in Fig. 5.

There is a clear deviation for ***o*-tol.-P3DMOT**, indicating that a methyl group on the 3-position of the monomer sidechain readily affects the controlled character of the polymerization. However, we observe that the impact on the controlled character of the polymerization is negligible at lower degrees of polymerization. These results are in line with earlier research investigating poly(3-alkylthiophene)s[20] and poly(3-alkyltelurophene)s[21] with branched sidechains.

Influence of the cat. initiator. To study the influence of the catechol-based external initiator, first a series of **cat.-P3HT** is synthesized from **3HT**, using **cat.**. From the GPC-obtained M_n vs $[M]_0/[I]$ plot (Fig. 5), we can conclude that the **cat.** initiator has no influence on the controlled character of the polymerization of **3HT**. Next, series of ***o*-tol.-P3DMOT** and **cat.-P3DMOT** are also synthesized. When comparing the GPC-obtained M_n *vs* $[M]_0/[I]$ evolution for these polymers, we notice that the data points of the latter deviate from the linear correlation at lower M_n: 15 kg/mol for **cat.-P3DMOT** *vs* 21 kg/mol, for ***o*-tol.-P3DMOT**. (Fig. 5) We conclude that termination and/or transfer reactions occur more frequently during the polymerization of **cat.-P3DMOT**, compared to that of **o-tol.-P3DMOT**, which can be attributed to the influence of the **cat.** initiator group. This is not surprising as it is known for more electron-rich groups to interact more with the propagating Ni-entity.[19] These results are backed-up by MALDI-ToF measurements (ESI), where we see that for **cat.-P3DMOT** significantly less catechol/H terminated chains are present with increasing M_n. This in contrast to the ***o*-tol.-P3DMOT** spectra, suggesting that more transfer reactions take place during the **cat.-P3DMOT** polymerization. Also notice that, since there is a linear correlation for the **cat.-P3HT** series, only the combination of the branched monomer with the catechol-based external initiator results in additional termination and/or transfer reactions, compared to the loss over the polymerization controlled character induced by the branched monomer alone.

We suggest the following mechanism to explain these findings. It is known that transmetalation is the rate-determination step during the polymerization of poly(3-alkylthiophene) when using dppp as the ligand for the propagating Ni-entity.[22] Hence, during the remaining stages of the polymerization cycle, the Ni-entity is oxidatively inserted in the terminal C-Br end of the growing polymer chain. (Fig. 6 **(A)**) However, as shown by a recent study, for more sterically demanding monomer sidechains, an equilibrium sets in between the oxidatively inserted catalyst **(A)** and the catalyst associated with the polymer chain **(B)**.[20] In this associated stage, the Ni-entity can ringwalk over the polymer chain, making dissociation and thus termination reactions more probable **(D)**.[23,24,25] Also can the Ni-entity migrate to the chain α-end to interact with the initiator functional group **(C)**. The stronger the interaction between the initiator functional group and the Ni-entity, the more the latter is trapped at the chain's α-end, preventing further chain growth and possibly leading to transfer or termination reactions **(D)**. Combining a decreased association with the sterically hindered thiophene units and a stronger interaction with the electron rich initiator group leads to a diminished control over the polymerization, especially for higher degrees of polymerization. When the interaction between the Ni-entity and the polymer chain is stronger than that with the initiator functional group, as is the case during the synthesis of **cat.-**

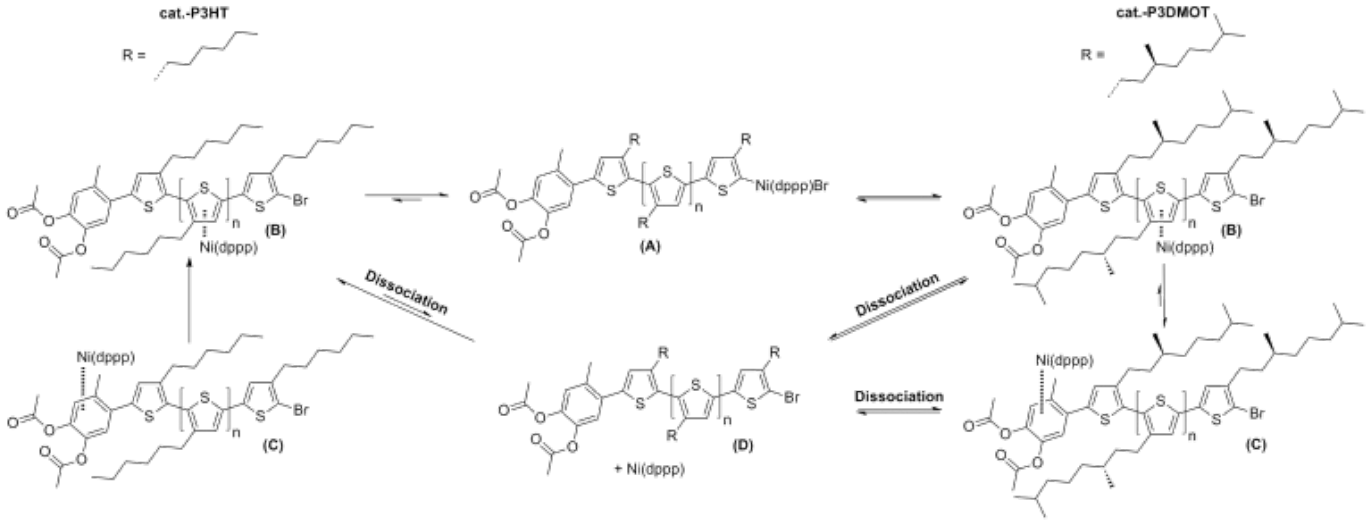

Fig. 6 Different stages in the **cat.** initiated polymerization of **3HT** and **3DMOT**.

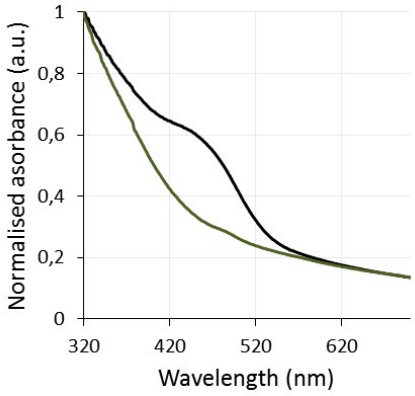

Fig. 7 UV/Vis spectra the Fe_3O_4 nanoparticles (green) and **Fe_3O_4-cat.-P3DMOT** (black) in THF at room temperature.

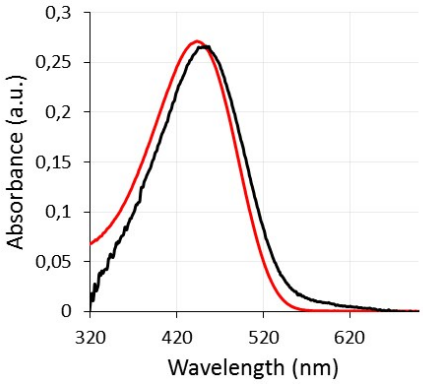

Fig. 8 UV/Vis spectrum of **cat.-P3DMOT** (red) in THF at room temperature and the calculated contribution of the polymer to the spectrum of the hybrid material (black).

P3HT, no trapping of the Ni by the catechol group occurs and the control over the polymerization is assured. Notice that this presents a new proof that ringwalking is a viable concept, since it is crucial to take place before the Ni-entity is able to interact with the catechol group.

Synthesis of the hybrid material. A **cat.-P3DMOT** of 8.4 kg/mol is chosen to be coupled to the magnetite nanoparticles. At this molar weight, the polymerization is still controlled and the obtained material presents well defined end-groups and a low polydispersity. The polymer is characterized by GPC, ^{1}H NMR, UV/Vis and MALDI-ToF analysis and shows a dispersity of 1.1 and an initiator incorporation of 96.8% (via ^{1}H NMR)[19]. The functionalization of the magnetite nanoparticles is a two-step one-pot reaction, where first the catechol functionality is activated by removing the protective acetyl groups which are necessary to make the initiator compatible with the Grignard reagents during the polymerization. For this deprotection, $NH_4(OH)$ is added in THF. Next, the strong interaction of the activated catechol functionality with the magnetite nanoparticle is the driving force in the exchange between the **cat.-P3DMOT** and the original oleic acid ligand. The obtained hybrid material **Fe_3O_4-cat.-P3DMOT** is purified through centrifugation and analyzed via UV/Vis, CD, AFM, TEM, TGA and Faraday measurements. We note that the methodology required is more challenging for the new catechol based than for a phenyl based initiator[19], as for the latter the deprotection and subsequent coupling with nanoparticles can be performed in separate steps. The presence of the polymer after functionalization and removal of uncoupled, free polymer is confirmed via UV/Vis of the samples dissolved in THF. The spectra of the hybrid material is compared with that of the magnetite nanoparticles (Fig. 7) and the contribution of the polymer in the spectrum of the hybrid material, calculated by subtracting the spectrum of the pure nanoparticles, is compared with that of the free polymer (Fig. 8).

Further, we compare the aggregational behavior of the hybrid material and **cat.-P3DMOT**. For this, UV/Vis spectra are recorded in different mixtures of good (THF) and poor (methanol) solvents. Since the aggregation of the polymer is concentration dependent, the initial polymer concentration in both samples is matched by equalizing the maximal polymer absorbance of the 100% THF solution (Fig. 8). Next, with an automated syringe, methanol is added to the rotating solution until THF-MeOH ratios of 10-0, 9-1, 8-2 etc. were obtained. The recorded spectra are corrected for the dilution effect and shown in Fig. 9 and Fig. 10. We note that the use of an automated syringe and identical methodologies for all prepared samples justifies the comparison of the obtained spectra of both materials, despite the gradual dilution of the samples.

The spectra of **cat.-P3DMOT** show typical poly(3-alkylthiophene) aggregation behavior in which the interchain pi-pi stacking induces more planarization and aggregation with increasing methanol concentration. This results in a red shift of lambda max starting from the 40% methanol spectrum. For the hybrid material, no red shift is observed, but tailing occurs in the 30% methanol spectrum, potentially indicating the start of planarization. This difference in aggregation behavior is an additional proof that the polymer is attached to the magnetite nanoparticles, and that this attachment obstructs the stacking of the polymer chains. Also, we can assume a successful functionalization and subsequent purifications, as free polymer

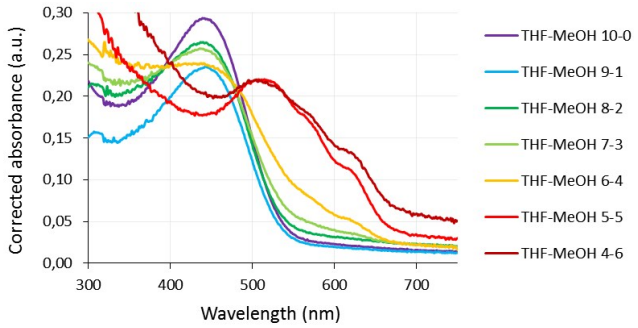

Fig. 9 UV/Vis spectra of **cat.-P3DMOT** in several THF-MeOH mixtures at room temperature.

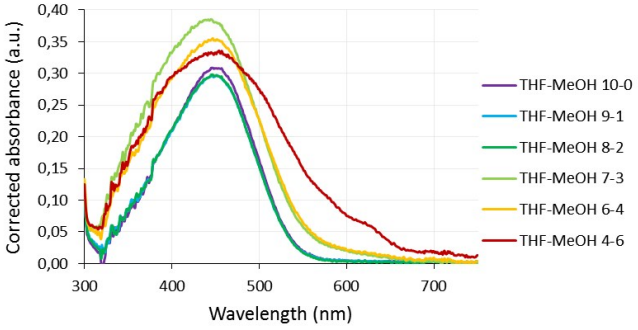

Fig. 10 UV/Vis spectra of **Fe_3O_4-cat.-P3DMOT** in several THF-MeOH mixtures at room temperature.

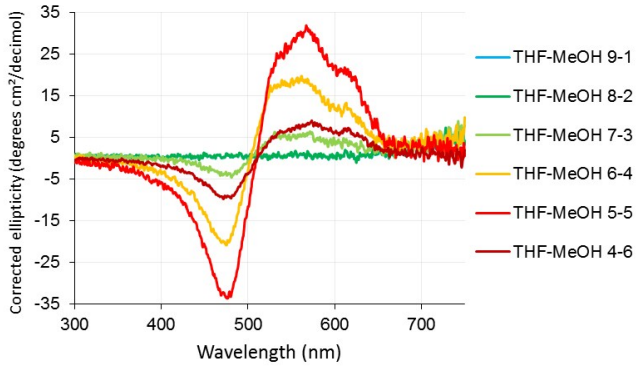

Fig. 11 CD spectra of **cat.-P3DMOT** in several THF-MeOH mixtures at room temperature.

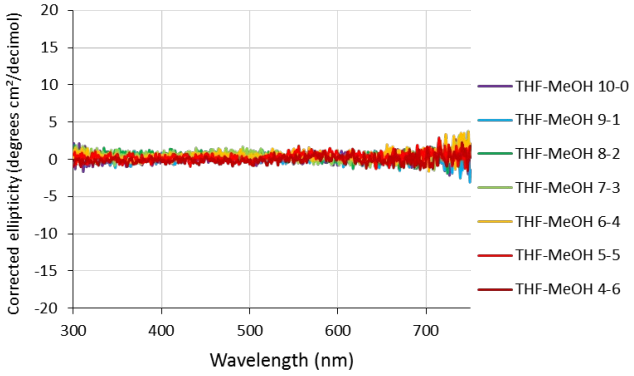

Fig. 12 CD spectra of **Fe_3O_4-cat.-P3DMOT** in several THF-MeOH mixtures at room temperature.

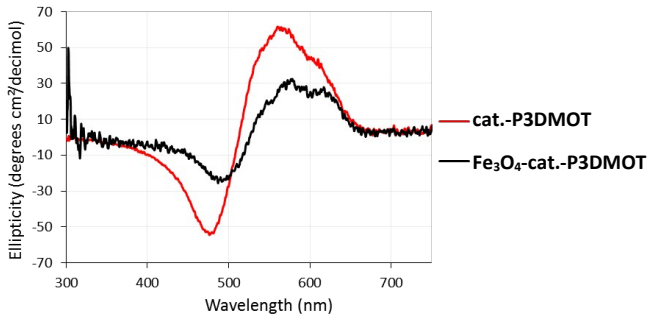

Fig. 13 CD spectra of **cat.-P3DMOT** (red) and **Fe_3O_4-cat.-P3DMOT** (black) in film in THF at room temperature.

would result in the appearance of a second peak, comparable with the one of **cat.-P3DMOT**.

The supramolecular ordering is further investigated via CD-measurements of samples in different THF-MeOH mixtures prepared similar as described previously. Additional to this, spin coated films are prepared from solutions in chloroform and measured. During spin coating of all samples on degreased (*i*-PrOH) glass substrates, a maximum of 800 rpm is reached after 3 seconds and this speed is maintained for 15 seconds. The CD-spectra of **cat.-P3DMOT** in solution show a bisignate Cotton effect starting at a methanol concentration of 30%, while the UV/Vis spectra only show a red shift from 40% methanol (Fig. 11). This can be explained by the formation of small chiral aggregates at 30%, which the CD-detector is capable of detecting, but that give no significant UV/Vis-signal. The intensity of the CD-signal increases with the amount of aggregated polymer, but diminishes as the sample is diluted with methanol. The fact that the spectrum at 60% methanol is less intense than that at 40% is probably due to the dilution effect surpassing the gain in intensity caused by the growth of the aggregates, which can be assumed to decrease towards the later stages of aggregation. For **Fe_3O_4-cat.-P3DMOT** no CD-signal is observed in solution (Fig. 12).

In film, **cat.-P3DMOT** and **Fe_3O_4-cat.-P3DMOT** show similar CD signals, but the spectrum of the latter is slightly redshifted and is less intense (Fig. 13). Since the UV/Vis spectra of **cat.-P3DMOT** and the calculated contribution of the polymer in **Fe_3O_4-cat.-P3DMOT** (Fig. 14) show similar intensities (Fig. 15), the diminished CD signal of **Fe_3O_4-cat.-P3DMOT** can be attributed to less chiral ordering in this sample, and not to a diminished absorption of the polymer. Here, also the blueshift of the polymer in **Fe_3O_4-cat.-P3DMOT** compared to the free **cat.-P3DMOT** indicates a decreased planarization and overlap of the polymer pi-orbitals caused by the attachment to the nanoparticles. Also the difference in shape could be attributed to the coupling to the nanoparticles.

When the polymer is attached to the nanoparticles, two forms of interchain interaction can be proposed; (1) interaction between chains on the same nanoparticle and (2) interaction between chains on different nanoparticles (Fig. 16). No CD-signal is present for the hybrid nanoparticles in solution. Therefore, interactions between polymer chains attached to the same nanoparticle can be excluded, since these are concentration independent and would occur in poor solvent even at low concentrations. Knowing that even a short

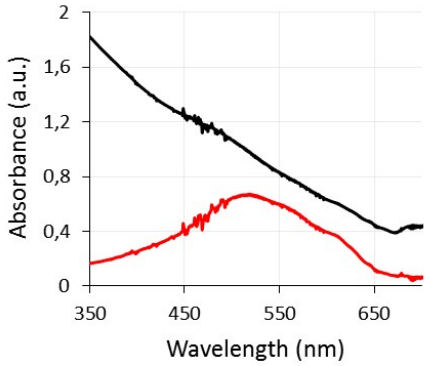

Fig. 14 UV/Vis spectra of **cat.-P3DMOT** (red), **Fe_3O_4-cat.-P3DMOT** (black) in THF at room temperature.

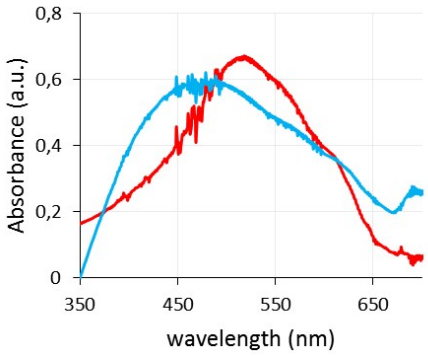

Fig. 15 UV/Vis spectra of **cat.-P3DMOT** (red) and the calculated contribution of the polymer in **Fe_3O_4-cat.-P3DMOT** (blue) in THF at room temperature.

View Article Online
DOI: 10.1039/C8PY00595A

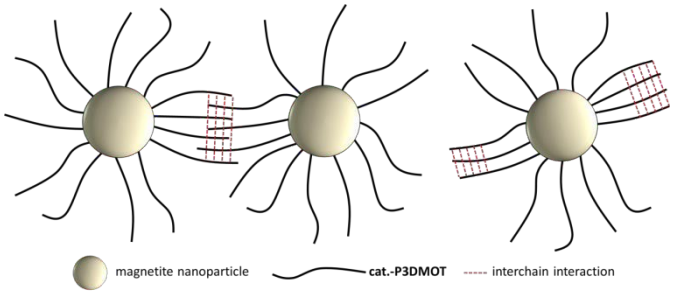

Fig. 16 Two forms of possible interchain interaction in **Fe_3O_4-cat.-P3DMOT**.

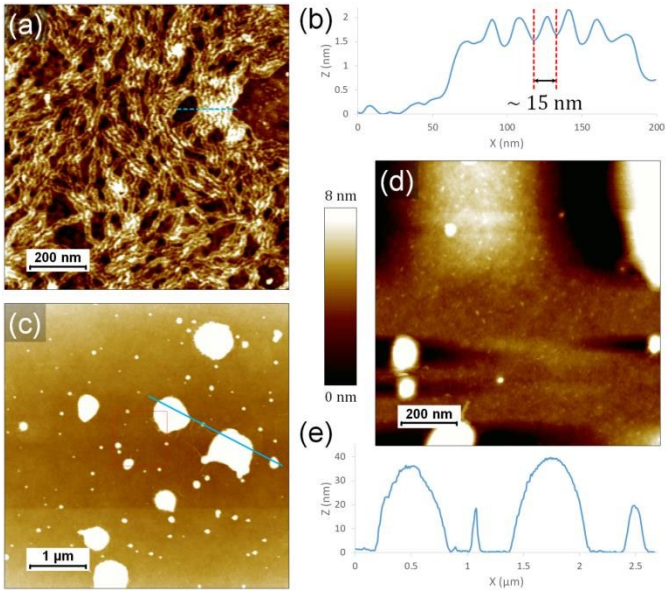

Fig. 17 AFM topography images of **cat.-P3DMOT** (a) and **Fe_3O_4-cat.-P3DMOT** (c, d). Line profiles (b, e) along the blue lines in panels (a) and (c), respectively. Image (d) corresponds to the region within the red square in panel (c).

range chiral ordering already gives rise to a significant CD-response, the CD-signal in film indicates some form of interchain interaction. Interactions between polymer chains of different nanoparticles are probable and would explain the presence of a CD-signal in film, but not in solution, since the evaporation of the solvent during spin coating could induce interchain interactions by bringing the nanoparticles together. From these UV/Vis- and CD-results we can conclude that only interactions between chains on different nanoparticles emerge upon aggregation in our hybrid system.

For determining the range of the interchain interactions AFM measurement of the **cat.-P3DMOT** and hybrid material films are conducted. The topography of both types of films is imaged using the intermittent contact mode. The **cat.-P3DMOT** is organized in fibers wide of 15-20 nm, typical of self-assembled polyalkylthiophenes.[26] In this organization, the planarized polymer chains are perpendicular to the main axis of the fibers and are assembled via pi-pi stacking. The functionalized nanoparticles appear as clusters of variable sizes, from 70 nm up to 600 nm in diameter (Fig. 17). The dimensions of the bigger clusters suggest they are formed by laterally aggregated nanoparticles (their height is on the other hand compatible with the size of a single nanoparticle), since a functionalized nanoparticle would have a diameter around 100 nm, based on the size of the magnetite nanoparticles and the polymer. Fibrilar structures are not observed on the clusters, which is not surprising since *i)* the roughness of the latter make the observation of the fibers more challenging and *ii)* UV-vis observations suggest that the attachment on the nanoparticles perturbs the chain stacking which is the driving force the fibers formation. The absence of fibers on the rest of the surface confirms in addition that there is no significant amount of free polymer in our samples. Since we observe many little clusters, long range ordering is improbable, but could to some extend be present in the larger aggregates.

Additional, to the AFM measurements, also TEM measurements of the magnetite nanoparticles and the hybrid material were conducted (ESI). For **Fe_3O_4-cat.-P3DMOT**, no polymer could be visualised, due to resolution issues caused by the high contrast of the magnetite nanoparticles. This is also observed in other studies.[9] Further also TGA measurements of **Fe_3O_4-cat.-P3DMOT** were conducted (ESI). After heating to 545.81 °C, it can be concluded that the remaining 15 weight% consist of the magnetite nanoparticle cores and thus, that the hybrid material contains about 85 weight% of polymer.[9]

To verify the range of the supramolecular ordering in the materials, Faraday measurements are performed on the spin-coated films. Faraday-rotation in poly(3-alkylthiophene) relies on long range ordering of the polymer chains.[27,28] The **cat.-P3DMOT** is compared with the reference glass and indeed a contribution of the polymer is observed, confirming supramolecular order in this

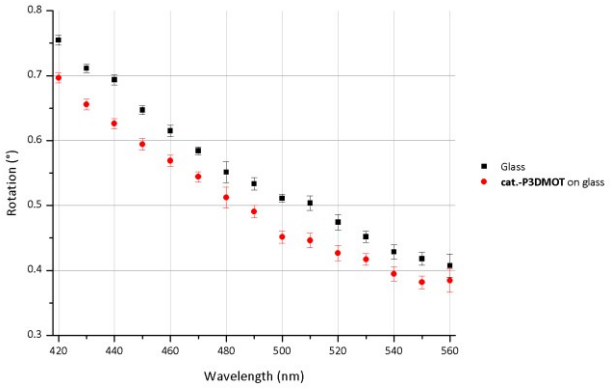

Fig. 18 Faraday measurement of **cat.-P3DMOT**.

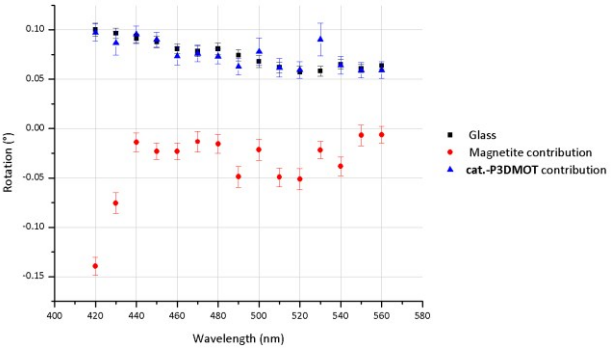

Fig. 19 Faraday measurement of the hybrid material **Fe_3O_4-cat.-P3DMOT**.

sample (Fig. 18). Also the hybrid material is measured and the contributions of the magnetite nanoparticle and the polymer are calculated (Fig. 19) (ESI). We observe that here the Faraday rotation is solely originating from the nanoparticles and that the ordering of the polymer is too disrupted to give a detectable Faraday signal. We conclude that no long distance ordering is present in the hybrid material.

Conclusion

Low dispersity poly((*S*)-3-(3',7'-dimethyloctyl)thiophene) presenting targeted molar mass and end-groups is synthesized via KCTCP, using the **cat.** catechol-based external Ni-initiator. First it is investigated to which extend the controlled character of the KCTCP is preserved when polymerizing the branched (+)-(*S*)-2-bromo-5-chloromagnesio-3-(3,7-dimethyloctyl)thiophene (**3DMOT**) monomer or when using **cat.**. When polymerizing **3DMOT** with an ***o*-tol.** initiator, it is found that a methyl group on the 3-position of the monomer sidechain already affects the controlled character of the polymerization. When investigating the influence of **cat.** on the polymerization of 2-bromo-5-chloromagnesio-3-hexylthiophene **3HT** and **3DMOT**, we notice that the polymerization of 3HT with **cat.** is controlled until at least 27 kg/mol. On the other hand, the combination of the branched monomer with the catechol-based external initiator results in an additional loss over the polymerization controlled character compared to the polymerization of **3DMOT** with ***o*-tol.**. A hypothesis to explain these findings is given. Both the effect of the branched monomer and the **cat.** initiator on the controlled character of the polymerization are negligible at lower degrees of polymerization. Next, **cat.-P3DMOT** is coupled to magnetite nanoparticles and the obtained hybrid material is investigated. Via CD, UV/Vis, AFM and Faraday measurements, we conclude that no long range supramolecular ordering is present in the **Fe_3O_4-cat.-P3DMOT** hybrid material and that only interchain interactions between polymer chains attached on different nanoparticles are present.

Conflicts of interest

There are no conflicts to declare.

Acknowledgements

We are grateful to the Onderzoeksfonds KU Leuven/Research Fund KU Leuven, IWT-SBO and the Fund for Scientific Research (FWO Vlaanderen) for financial support. W.C. is grateful to IWT for a doctoral fellowship. Research in Mons is supported by the Science Policy Office of the Belgian Federal Government (PAI 7/5), the European Commission/Region Wallonne FEDER program, and the "Fonds National pour la Recherche Scientifique" (FRS-FNRS).

Notes and references

1 L. Verheyen, P. Leysen, M.-P. Van Den Eede, W. Ceunen, T. Hardeman and G. Koeckelberghs, *Polymer (Guildf).*, 2017, **108**, 521–546.
2 L. Vinet and A. Zhedanov, *Chem. Rev.*, 2010, **107**, 1324–1338.
3 C. J. Brabec, N. S. Sariciftci and J. C. Hummelen, *Adv. Funct. Mater.*, 2001, **11**, 15–26.
4 H. Borchert, *Energy Environ. Sci.*, 2010, **3**, 1682.
5 J. Liu, T. Tanaka, K. Sivula, a P. Alivisatos and J. M. J. Fréchet, *J. Am. Chem. Soc.*, 2004, **126**, 6550–1.
6 K. Palaniappan, J. W. Murphy, N. Khanam, J. Horvath, H. Alshareef, M. Quevedo-Lopez, M. C. Biewer, S. Y. Park, M. J. Kim, B. E. Gnade and M. C. Stefan, *Macromolecules*, 2009, **42**, 3845–3848.
7 W. M. Kochemba, D. L. Pickel, B. G. Sumpter, J. Chen and S. M. Kilbey, *Chem. Mater.*, 2012, **24**, 4459–4467.
8 R. A. Krüger, T. J. Gordon, T. Baumgartner and T. C. Sutherland, *ACS Appl. Mater. Interfaces*, 2011, **3**, 2031–2041.
9 Y. Lin, J. Chu, H. Lu, N. Liu and Z. Wu, *Macromol. Rapid Commun.*, 2018, **39**, 1700685.
10 S. Aute, P. Maity, A. Das and H. N. Ghosh, *New J. Chem.*, 2017, **41**, 5215–5224.
11 Y. Ooyama, T. Yamada, T. Fujita, Y. Harima and J. Ohshita, *J. Mater. Chem. A*, 2014, **2**, 8500.
12 A. Smeets, P. Willot, J. De Winter, P. Gerbaux, T. Verbiest and G. Koeckelberghs, *Macromolecules*, 2011, **44**, 6017–6025.
13 A. K. L. Yuen, G. a Hutton, A. F. Masters and T. Maschmeyer, *Dalton Trans.*, 2012, **41**, 2545–59.
14 P. Singhal, P. Maity, S. K. Jha and H. N. Ghosh, *Chem. - A Eur. J.*, 2017, **23**, 10590–10596.
15 E. Amstad, T. Gillich, I. Bilecka, M. Textor and E. Reimhult, *Nano Lett.*, 2009, **9**, 4042–8.
16 H. Awada, L. Mezzasalma, S. Blanc, D. Flahaut, C. Dagron-Lartigau, J. Lyskawa, P. Woisel, A. Bousquet and L. Billon, *Macromol. Rapid Commun.*, 2015, **36**, 1486–1491.
17 W. J. E. Beek, M. M. Wienk and R. A. J. Janssen, *Adv. Funct. Mater.*, 2006, **16**, 1112–1116.
18 K. Van den Bergh, J. Huybrechts, T. Verbiest and G. Koeckelberghs, *Chemistry*, 2008, **14**, 9122–9125.
19 F. Monnaie, W. Brullot, T. Verbiest, J. De Winter, P. Gerbaux, A. Smeets and G. Koeckelberghs, *Macromolecules*, 2013, **46**, 8500–8508.
20 L. Verheyen, B. Timmermans and G. Koeckelberghs, *Polym. Chem.*, 2017, **8**, 2327–2333.
21 S. Ye, M. Steube, E. I. Carrera and D. S. Seferos, *Macromolecules*, 2016, **49**, 1704–1711.
22 E. L. Lanni and A. J. McNeil, *Macromolecules*, 2010, **43**, 8039–8044.
23 T. Beryozkina, V. Senkovskyy, E. Kaul and A. Kiriy, *Macromolecules*, 2008, **41**, 7817–7823.
24 A. Kiriy, V. Senkovskyy and M. Sommer, *Macromol. Rapid Commun.*, 2011, **32**, 1503–1517.
25 R. Tkachov, V. Senkovskyy, H. Komber, J.-U. Sommer and A. Kiriy, *J. Am. Chem. Soc.*, 2010, **132**, 7803–7810.
26 P. Willot, J. Steverlynck, D. Moerman, P. Leclère, R. Lazzaroni and G. Koeckelberghs, *Polym. Chem.*, 2013, **4**, 2662.
27 P. Gangopadhyay, R. Voorakaranam, A. Lopez-Santiago, S. Foerier, J. Thomas, R. a. Norwood, A. Persoons and N. Peyghambarian, *J. Phys. Chem. C*, 2008, **112**, 8032–8037.
28 P. Gangopadhyay, G. Koeckelberghs and A. Persoons, *Chem. Mater.*, 2011, **23**, 516–521.

View Article Online
DOI: 10.1039/C8PY00393A

FOR TABLE OF CONTENTS ONLY

Fe_3O_4 nanoparticles decorated with a conjugated polymer is synthesized and the supramolecular organization of the polymer is studied.